Structural Engineering and Mechanics, Vol. 13, No. 2 (2002) 155-170

DOI: http://dx.doi.org/10.12989/sem.2002.13.2.155

Mixed finite element formulation for folded plates

Nihal Eratlı† and A. Yalçın Aköz‡

Faculty of Civil Engineering, Istanbul Technical University, 80626 Maslak-Istanbul,Turkey

Abstract. In this study, a new functional is obtained for folded plates with geometric (kinematic) and dynamic (natural) boundary conditions. This functional is the combination of two different functionals. Both functionals are obtained for thick plates which carry in-plane and lateral forces. A new mixed finite element is developed with 4×13 nodal parameters for folded plates (REC52). Forces and moments which are the necessary unknowns in engineering problems are obtained directly using the technique suggested here. The use of the global co-ordinate system causes time consuming operations and therefore the Lagrange multiplier method is used to relate the components of the parameters on the fold line. Numerical results are presented for folded plates and compared with experimental results.

Key words: Reissner plate; folded plate; mixed-finite element.

1. Introduction

Folded plates are surface structures made from individual plane surfaces in which the thicknesses are smaller compared to other dimensions. The folded plates, which are constructed from rectangular plates are called prismatic folded plates, so their cross-sections are constant throughout their lengths. If the cross-section varies throughout the length, it is called non-prismatic folded plate. The plates can individually be either prismatic or non-prismatic, but then the whole system is termed non-prismatic. Folded plates are formed as multiple bay or multispan construction systems. The intersection lines between individual plates are usually termed as fold lines.

The folded plates find wide application in engineering field. Naturally, there exist many studies in the literature. Supplementary information about solution methods of folded plates are given in Report of Task Committee (1963), Iffland (1979), Rockey and Evans (1967), Lavy *et al*. (1992), Ohga *et al.* (1991).

The solution of folded plates problem is based on thin plate theory. To provide a more reliable representation of plates, several refined theories which consider transverse shear strain are introduced (Reissner 1946, Mindlin 1951). Displacement type elements have been established employing Reissner-Mindlin plate theories. The finite element formulation based on these methods requires C^0 continuity, in which a problem known as “Shear Locking” is encountered, when the plate thickness approaches zero (Zienkiewicz *et al.* 1977, Pugh *et al.* 1978). To the best of the author’s knowledge, two basic approaches are suggested in the literature to avoid shear locking in thin plate problems. These are uniform reduced integration/selective reduced integration schemes (Zienkiewicz *et al.* 1971, Hughes *et al.* 1977, Belytschko *et al.* 1981) and discrete Kirchhoff plate

† Associate Professor
‡ Professor

theory (DKT) (Katılı 1993a, b). When displacement type elements are used, there is a need, also, for additional computations to obtain internal forces. It is a well known fact that the numerical differentiation magnifies errors. At the same time, the internal forces obtained by these methods are discontinuous at the nodes.

Recently, Eratlı and Aköz (1997) developed the REC32 and TR48 elements using Gâteaux approaches. Convergence tests on this method show that these elements are free from shear locking. Also all internal forces are obtained directly and they are continuous at nodes.

A new functional is presented in this paper, it is obtained combining the separate functionals for Reissner plate and in-plane plate elements presented in Eratlı Uzcan (1995) using the Gâteaux approach, Reddy (1986). For a relatively simple problem, the functional can be obtained using the Hellinger-Reissner and Hu-Washizu principles. However, Gâteaux differential approaches have some important advantages. They ensure, in particular, the consistency of the field equations. This subject is discussed in detail in Aköz and Özütok (2000).

This functional includes the necessary dynamic (natural) and geometric (kinematic) boundary conditions. A literature survey has not revealed a similar functional which is also transformable to the classical energy equations. As the functional involves only first derivatives on the variables, linear interpolation functions satisfy completeness and continuity requirements, Eratlı and Aköz (1997). A global co-ordinate system is necessary to express the parameters assigned to different plates. The use of the global co-ordinate system causes time consuming operations. Therefore, the Lagrange multiplier method is used to relate the components of the parameters on the fold lines which have been expressed in two different plate co-ordinate systems. All these relations are included in the functional through Lagrange multipliers. The element matrix thus obtained is applied to folded plate problems. Numerical results are presented for folded plates and are compared with experimental results.

2. Functional for folded plates

The field and boundary equations for thick plates carrying lateral and in-plane loads, Eqs. (1-3) and Eqs. (4-6), respectively, Panc (1975), Eratlı Uzcan (1995), Eratlı and Aköz (1997), are summarised below for the reference systems shown in Figs. 1-2 and for the notation given in Appendix II:

$$\frac{\partial M_x}{\partial x} + \frac{\partial M_{xy}}{\partial y} - Q_x = 0$$

$$\frac{\partial M_{xy}}{\partial x} + \frac{\partial M_y}{\partial y} - Q_y = 0$$

$$\frac{\partial Q_x}{\partial x} + \frac{\partial Q_y}{\partial y} + q = 0 \tag{1a}$$

$$\frac{\partial \Omega_x}{\partial x} - \frac{12}{Eh^3}\left(M_x - \mu M_y - \frac{h^2}{10}\mu q\right) = 0 \, (*)$$

$$\frac{\partial \Omega_y}{\partial y} - \frac{12}{Eh^3}\left(M_y - \mu M_x - \frac{h^2}{10}\mu q\right) = 0 \tag{1b}$$

(*) See the Appendix I.

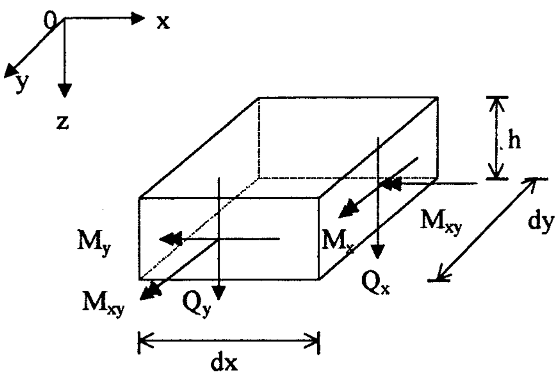

Fig. 1 Internal forces for plate element

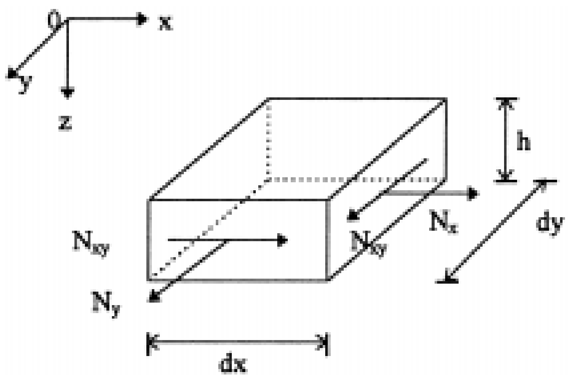

Fig. 2 Internal forces for in-plane element

$$\frac{\partial \Omega_x}{\partial y} + \frac{\partial \Omega_y}{\partial x} - \frac{12}{Gh^3} M_{xy} = 0$$

$$\Omega_x + \frac{\partial w}{\partial x} - \frac{6}{5Gh} Q_x = 0$$

$$\Omega_y + \frac{\partial w}{\partial y} - \frac{6}{5Gh} Q_y = 0. \tag{1c}$$

$$\boldsymbol{M} - \hat{\boldsymbol{M}} = 0$$

$$\boldsymbol{Q} - \hat{\boldsymbol{Q}} = 0, \tag{2}$$

$$-\boldsymbol{w} - \hat{\boldsymbol{w}} = 0$$

$$-\boldsymbol{\Omega} - \hat{\boldsymbol{\Omega}} = 0. \tag{3}$$

$$\frac{\partial N_x}{\partial x} + \frac{\partial N_{xy}}{\partial y} + p = 0 \tag{4a}$$

$$\frac{\partial N_{xy}}{\partial x} + \frac{\partial N_y}{\partial y} + r = 0 \tag{4b}$$

$$N_x - \frac{Eh}{1-\mu^2}\left[\frac{\partial u}{\partial x} + \mu \frac{\partial v}{\partial y}\right] = 0 \tag{4c}$$

$$N_y - \frac{Eh}{1-\mu^2}\left[\frac{\partial v}{\partial y} + \mu \frac{\partial u}{\partial x}\right] = 0 \tag{4d}$$

$$N_{xy} - \frac{Eh}{2(1+\mu)}\left[\frac{\partial u}{\partial y} + \frac{\partial v}{\partial x}\right] = 0\,. \tag{4e}$$

$$-\boldsymbol{N} + \hat{\boldsymbol{N}} = 0, \tag{5}$$

$$\boldsymbol{u} - \hat{\boldsymbol{u}} = 0. \tag{6}$$

$\boldsymbol{M}$, $\boldsymbol{Q}$, $\boldsymbol{\Omega}$ and $\boldsymbol{w}$ are the moment, force, rotation and deflection vectors for the bending element and $\boldsymbol{N}$, $\boldsymbol{u}$, $\boldsymbol{v}$ are the force and deflection vectors for the in-plane element. In Eqs. (2) and (3) quantities with " ^ " are known values on the boundary. A functional for the Reissner plate (I_p) is obtained by Aköz-Uzcan (Eratlı) (1992) using the functional analysis method and the Gâteaux differential. The mathematical procedure is explained in detail in Aköz *et al.* (1991).

$$
\begin{aligned}
I_p(y) = {} & [Q_x,(\Omega_x + w_{,x})] + [Q_y,(\Omega_y + w_{,y})] + [M_x,\Omega_{x_{,x}}] + [M_y,\Omega_{y_{,y}}] + [M_{xy},\Omega_{x_{,y}}] \\
& + [M_{xy},\Omega_{y_{,x}}] - \frac{6}{Eh^3}\{[M_x,M_x] + [M_y,M_y] - 2\mu[M_x,M_y] + 2(1+\mu)[M_{xy},M_{xy}]\} \\
& - \frac{3}{5Gh}\{[Q_x,Q_x] + [Q_y,Q_y]\} + \frac{6\mu}{5Eh}\{[q,M_x] + [q,M_y]\} - [q,w] - [(w - \hat{w}),Q]_\varepsilon \\
& - [(\Omega - \hat{\Omega}),M]_\varepsilon - [w,\hat{Q}]_\sigma - [\hat{M},\Omega]_\sigma,
\end{aligned}
\tag{7}
$$

A second functional is obtained for in-plane elements (I_l) in Eratlı Uzcan (1995).

$$
\begin{aligned}
I_l(y) = {} & [N_x,u_{,x}] + [N_y,v_{,y}] + [N_{xy},v_{,x}] + [N_{xy},u_{,y}] + \frac{1}{2Eh}[N_x,N_x] + \frac{1}{2Eh}[N_y,N_y] \\
& - \frac{\mu}{Eh}[N_x,N_y] + \frac{(1+\mu)}{Eh}[N_{xy},N_{xy}] - [p,u] - [r,v] - [\hat{N}_x,u]_\sigma - [\hat{N}_y,v]_\sigma \\
& - [\hat{N}_{xy},u]_\sigma - [\hat{N}_{xy},v]_\sigma - [(u - \hat{u}),N_x]_\varepsilon - [(v - \hat{v}),N_y]_\varepsilon - [(u - \hat{u}),N_{xy}]_\varepsilon \\
& - [(v - \hat{v}),N_{xy}]_\varepsilon .
\end{aligned}
\tag{8}
$$

The parentheses with subscripts σ and ε indicate the dynamic (natural) and the geometric (kinematic) boundary conditions, respectively.

The functional which is obtained by summation of the Eqs. (7) and (8) can be used to solve folded plate problems:

$$
I_{fp} = I_p + I_l \tag{9}
$$

The stationary conditions of the proposed functionals yield the original equations. This variational operation is routine mathematical calculation, sake of simplicity, this calculation is not given here.

3. Isoparametric mixed finite element formulation of folded plates

In this section, the development of the finite element matrix for folded plates is presented. A four-noded rectangular element is used as shown in Fig. 3. The parent shape function corresponding to the i th nodal point is,

$$
\psi_i = \frac{1}{4}(1 + \xi\xi_i)(1 + \eta\eta_i), \qquad i = 1, ..., 4 \tag{10}
$$

where the subscripted non-dimensional parent coordinates take the values ± 1 at nodes of the element. These shape functions satisfy continuity and complement requirements, therefore the convergence requirements are satisfied (Huebner 1975).

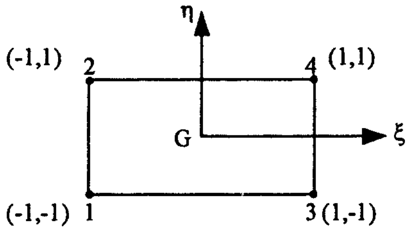

Fig. 3 Rectangular element

The nodal unknowns are the displacement components *u*, *v* and *w*, the normal forces N_x and N_y, the shear forces Q_x, Q_y and N_{xy}, the bending and torsion moments M_x, M_y and M_{xy} and the rotations of the cross-section, Ω_x and Ω_y. They are shown in Figs. 1 and 2. They lead to a 52 degrees of freedom element with 13 degrees of freedom per node (REC52). One of the important aims of the finite element method is that the error must converge to zero as the mesh is appropriately refined. The approximation requires the regularity (smoothness) and conformity element concepts. In this study, as the functional includes first order derivatives, the linear interpolation function satisfies the conformity requirements (Eratlı and Aköz 1997). The explicit form of the finite element matrix of the folded plate element REC52 is presented in Appendix III.

4. Application of finite element matrix to folded plates

The folded plate system which consists of a series of plane components can be divided into a number of plate elements. Each element is subjected to bending and in-plane stresses. The element matrix of folded plates can be established with respect to the plate co-ordinate system of each element. Adjacent plate elements are not coplanar. Therefore the displacements, forces and moments of each element must be expressed in a global co-ordinate system. The plate local co-ordinate system for each element is denoted by *x*, *y*, *z* and the global co-ordinate system for the complete folded plate is denoted by *X*, *Y*, *Z*. The two co-ordinate systems at the first node of a typical element are shown in Fig. 4.

Denoting by θ the angle between the *x* axis and the *X* axis, the displacements, forces and moments in the plate co-ordinate system can be expressed in the global co-ordinate system. The transformation at each node of the element is similar. Having carried out this transformation, for each element in turn, the element matrices are written in the appropriate format for the global co-ordinate system. The loads and boundary conditions are also involved in this transformation, and when the solution of folded plate is obtained, the results must be transformed back to the local plate co-ordinates. Therefore, this method is extremely time consuming.

In this study, the well known Lagrange Multiplier Method is applied to solve folded plate problems. The unknown parameters belonging to nodes on the fold line must be expressed in two different adjacent plate co-ordinate systems. Therefore, nodal values for these unknown parameters must be related by transformation as shown for displacements in Fig. 5. Furthermore, in this transformation, the component of the torsional moment perpendicular to the fold line yields a new component perpendicular to the plate surface. In the literature surveyed, this torsional component has been neglected for plate problems.

To inspect the effect of the lateral component of the concentrated torsional moments, an infinite

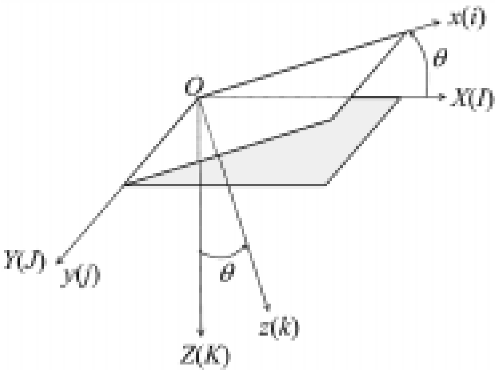

Fig. 4 Plate and global co-ordinate system

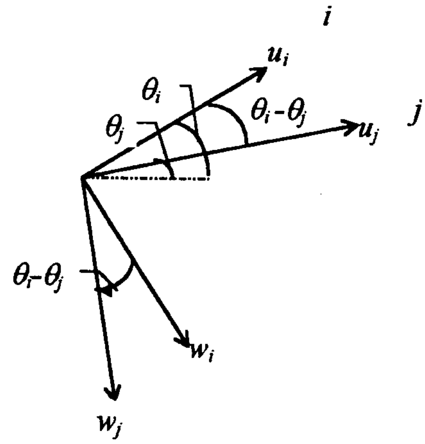

Fig. 5 Displacements in adjacent plates

plate is subjected to a perpendicular concentrated moment is inspected both theoretically and experimentally. This study, shows that:

· In a plate which is subject to a lateral torsional moment, the stresses and displacements are proportional to h^{-1}.

· In a plate subject to bending moment, the stresses and displacements are proportional to h^{-3}.

Therefore, when h is sufficiently small, the effects of lateral torsion can be neglected as in most applications reported in the literature. This effect is also verified for plates with various sizes and shapes by photoelastic experiments.

All these relations are included in the functional by the Lagrange multipliers in Eq. (11),

$$
\begin{aligned}
I_l = I_{fp} &+ \lambda_i(u_j - u_i \cos(\theta_i - \theta_j) - w_i \sin(\theta_i - \theta_j)) \\
&+ \lambda_j(w_j + u_i \sin(\theta_i - \theta_j) - w_i \cos(\theta_i - \theta_j)) \\
&+ \lambda_k(N_{xj} - N_{xi} \cos(\theta_i - \theta_j) - Q_{xi} \sin(\theta_i - \theta_j)) \\
&+ \lambda_l(Q_{xj} + N_{xi} \sin(\theta_i - \theta_j) - Q_{xi} \cos(\theta_i - \theta_j)) \\
&+ \lambda_m(N_{xy_j} - N_{xy_i} \cos(\theta_i - \theta_j) - Q_{yi} \sin(\theta_i - \theta_j)) \\
&+ \lambda_n(Q_{y_j} + N_{xy_i} \sin(\theta_i - \theta_j) - Q_{yi} \cos(\theta_i - \theta_j)).
\end{aligned} \tag{11}
$$

The enlarged global finite element matrix is established by extremizing the functional with respect to the nodal variables.

It is obvious that the Lagrange multiplier method is very simple in formulation and it save calculation time. To compare the Lagrange multiplier method and regular method, let us assume that M plates exist in folded plate ane each plate $m \times n$ element,

Number of total element (TEN) : $m \times n \times M$
Number of total unknown (TU) : $(m \times M+1) \times (n+1) \times 13$
Number of additional unknown for
the Lagrange multiplier method (AU) : $(M-1) \times m \times 6$
Number of additional (52×52) matrix
Transformation in regular method (MT) : $m \times n \times M$

If we compare MT times 52×52 matrix multiplication with an additional unknowns (AU), we can conclude that the Lagrange multiplier method is simpler than the regular transformation method.

5. Numerical examples

These section reports on examples solved with the REC52 mixed finite element presented above, and the solutions thus obtained are assessed using experimental results.

Example 1. Thin-thick plate validity limits and shear locking test

The transverse shears affect the plate behaviour as the plate thickness h is increase with respect to its length. Mindlin-Reissner plate theories must be used for the analysis of thick plates, which raises the question on the limit of validity of thin plate theory. To inspect the behaviour of the plate, a simply supported square plate subjected uniform load is solved for a varying thickness h (Fig. 6).

The deflection of the middle point of plate can be expressed as $w = \alpha\, q(2a)^4/Eh^3$. Coefficient α is given in literature, for the various ratios of b/a, Timoshenko and Woinowisky-Krieger (1959), e.g., $\alpha = 0.0443$ for $b/a = 1$ and thin plate theory. The results obtained using the formulation used here are presented in Table 1 for different $h/2a$ ratios. The graphs in Fig. 7 show that, the thin plate theory is valid for $h/2a \leq 0.1$. The numerical results are obtained for $h/2a = 0.001$ show that this formulation is free from shear locking. The convergence of this approach is studied in Aköz and Eratlı (2000).

Example 2. Folded plate with two elements

The dimensions of the second test structure are defined in Fig. 8. The thickness of plate is 0.2 cm. It is supported by a diaphragm along edges *FC*, *CA* and *ED*, *BD* and the horizontal sides *AB* and *EF* are free. This problem is solved using different meshes for the REC52 element. Reasonable convergence is obtained for the mesh shown in Fig. 9. The bending moments M_x, M_y at the centre cross-section are given in Fig. 10. The lateral displacements of the surface *ABCD* shown in Figs. 11 and 12 are obtained using program *SURFER* and the nodal displacement solutions of element REC52. A holographic test is performed to verify the numerical results for displacements. An aluminum folded plate is loaded by internal air pressure ($q = 0.196$ N/cm^2) and the model is

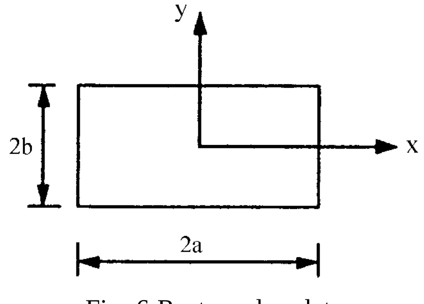

Fig. 6 Rectangular plate

Table 1 The coefficient α for different $h/2a$

$h/2a$	α
0.001	0.04496
0.002	0.04496
0.01	0.04501
0.02	0.04516
0.1	0.04936
0.2	0.05861
0.4	0.08468

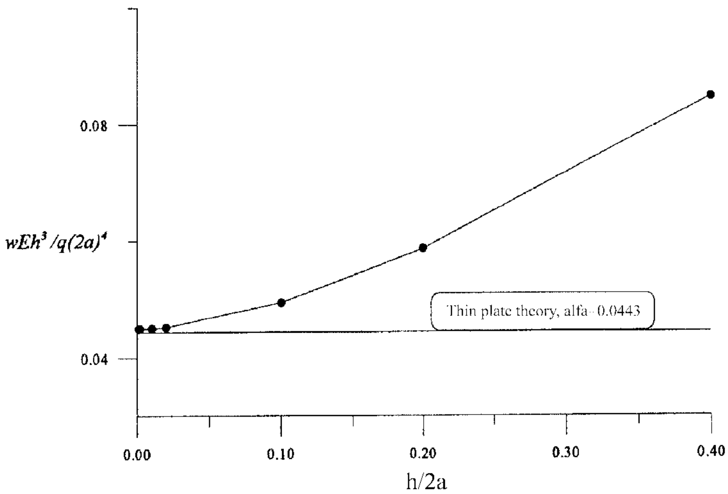

Fig. 7 Validity limits for thin plate

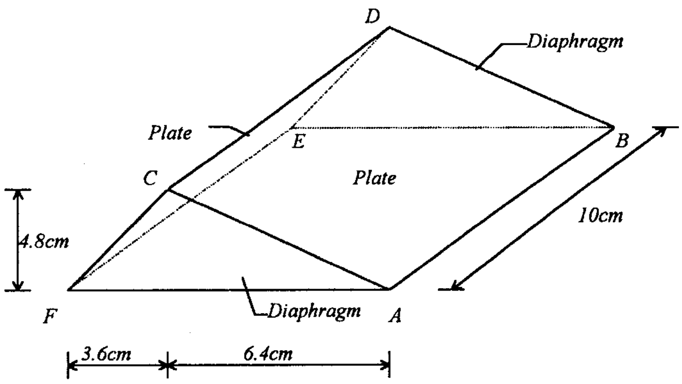

Fig. 8 Folded plate with two elements

illimunated by a 8 miliwatt He-Ne laser light. A double-exposure method is used in the experiment and the holographic picture is taken from Stroke (1968). The block diagram of arrangement for the holographic experiment is illustrated in Figs. 13 and 14. The fringes are the loci of the points having equal lateral displacements. Each fringe indicates a lateral displacement, Develis and

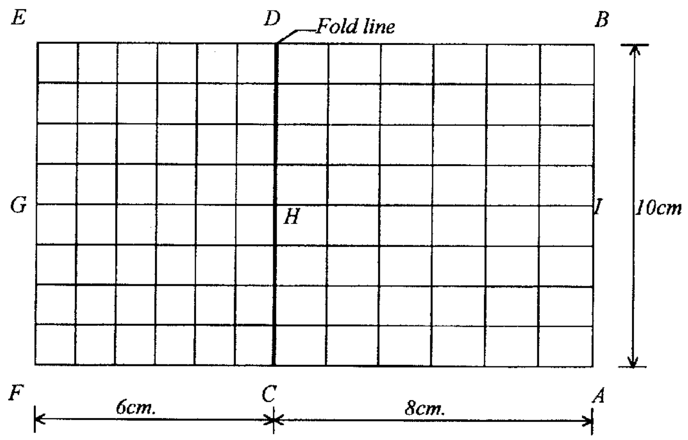

Fig. 9 Mesh size for folded plate with two elements

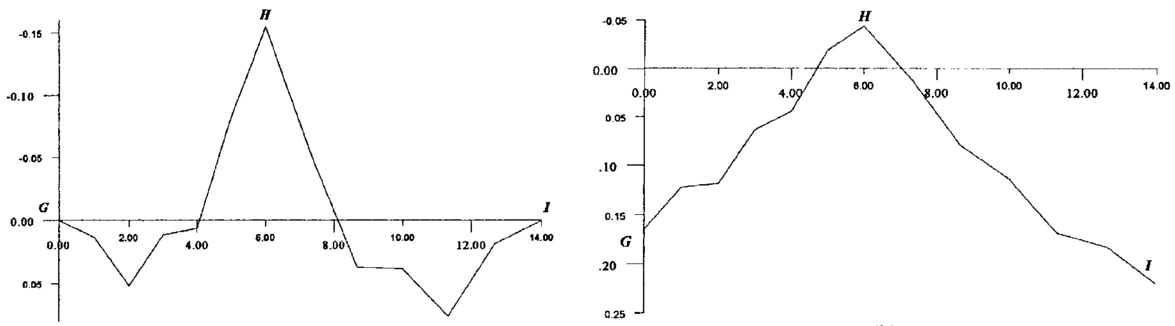

Fig. 10 M_x, M_y [Ncm/cm] bending moments along *GHI* centre cross-section line, respectively

Reynolds (1967),

$$w = \alpha\, n\, \lambda \tag{12}$$

where n is fringe number, λ is the wave-length of laser and α is the correction factor (α = 0.51-0.53), Eratlı Uzcan (1995). The wave-length of the He-Ne laser is 6328×10^{-8} cm. The numerical and experimental displacements are shown in Fig. 15. The results presented in Figs. 12, 14 and 15 show that the numerical and experimental results are in extremely good agreement. The effect of the thickness on the lateral displacement is also studied and the results obtained are given in Fig. 16. The pattern is similar to that reported in Fig. 7.

Example 3. Folded plate with three elements

The performance of the REC52 element in further assessed using the plate shown in Fig. 17. The problem is solved for different meshes and a reasonable convergence is obtained for the mesh shown in Fig. 18. The bending moments M_x, M_y at the centre cross-section are presented in Fig. 19. An aluminum folded plate is fabricated in size illustrated in Figs. 17 and 18. Several 120Ω *HH* strain-gauges (*PL*-5-11 *Q*.10 *G.L.* = 5 mm) are bounded at the points underneath the plate in the *x*

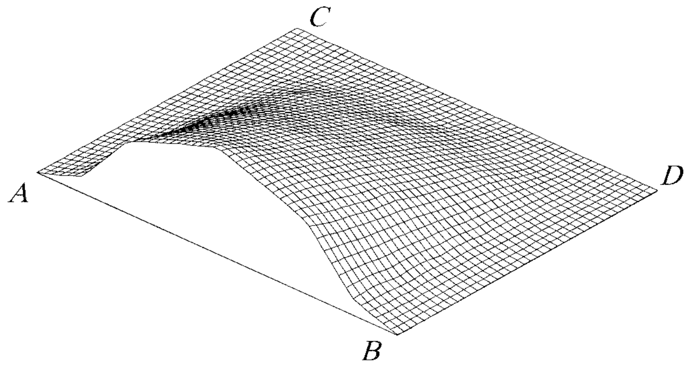

Fig. 11 Perspective view of displacement for *ABCD* part of folded plate with two elements

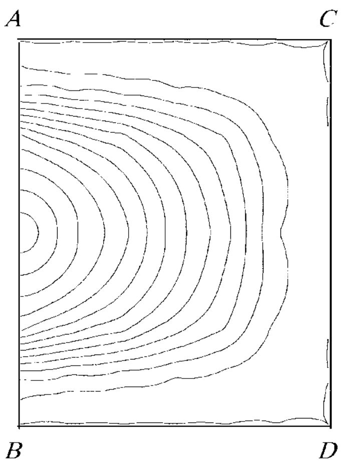

Fig. 12 Contour lines for *ABCD* part of folded plate with two elements

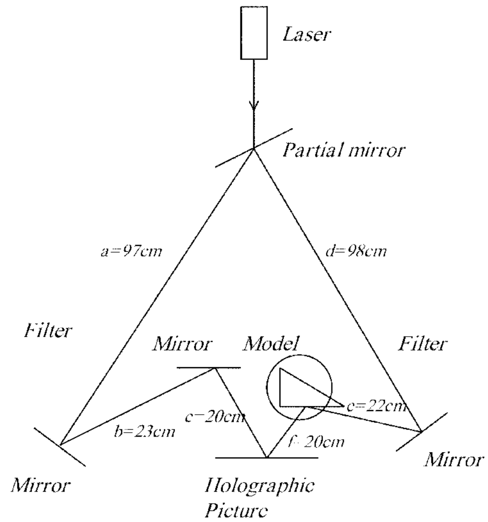

Fig. 13 Block diagram of holographic arrangement

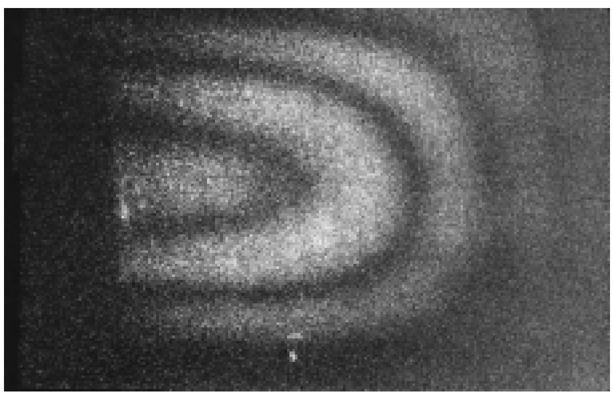

Fig. 14 Holographic picture

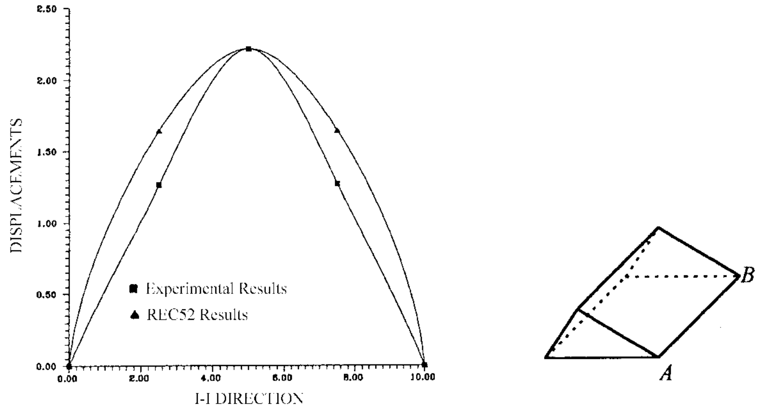

Fig. 15 Displacements along *AB* edge

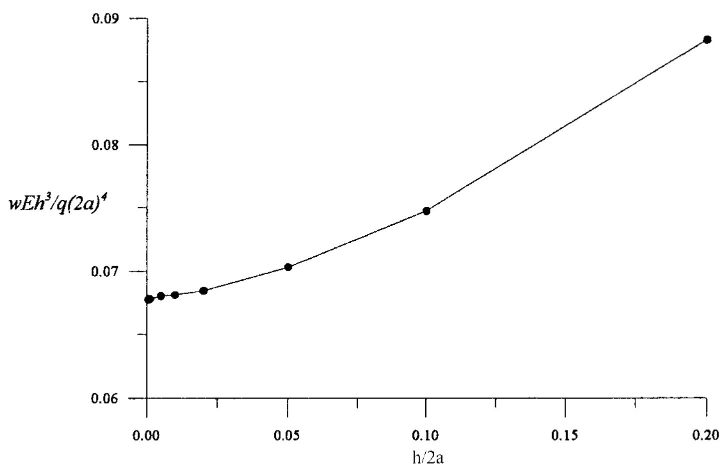

Fig. 16 The effects of the thickness on the displacement at the point *I*

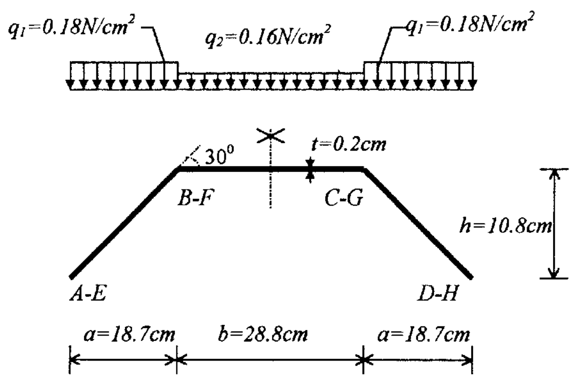

Fig. 17 Folded plate with three elements

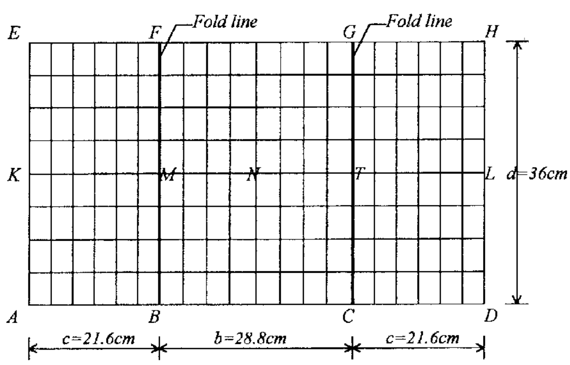

Fig. 18 Mesh size for folded plate with three elements

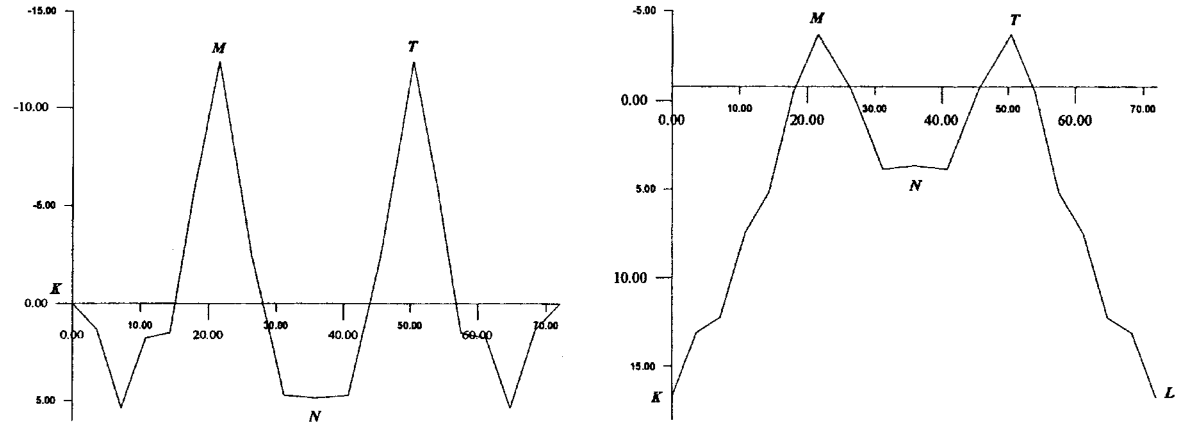

(a) (b)

Fig. 19 M_x, M_y [Ncm/cm] bending moments along *KMNTL* centre cross-section line, respectively

Table 2 Comparison of REC52 and experimental results

	ε_x		ε_y	
Points	REC52	Experiment	REC52	Experiment
M	70×10^{-6}	78×10^{-6}	49×10^{-6}	50×10^{-6}
N	-302×10^{-6}	-265×10^{-6}	-6×10^{-6}	-7×10^{-6}

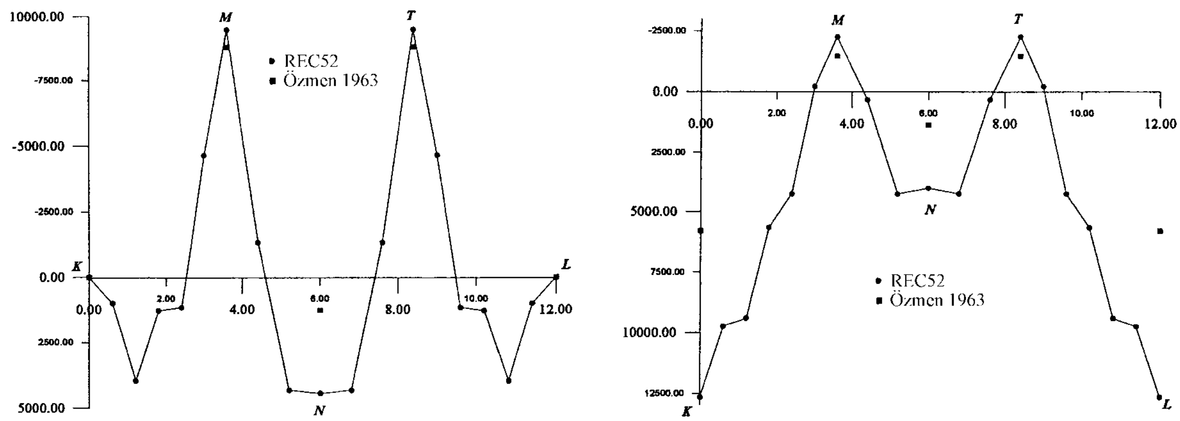

(a) (b)

Fig. 20 M_x, M_y [Nm/m] bending moments along *KMNTL* centre cross-section line, respectively

and y directions. The Young's modulus for the aluminum is obtained as 7×10^6 N/cm^2 by a calibration test. For the sake of simplicity, only the results obtained at the two main points are shown in Table 2.

The same structure with different dimensions is studied by Özmen (1963): $q_1 = 5.28$ N/m^2,

q_2= 4.81 N/m^2, a = 3.118 m, b = 4.8 m, c = 3.6 m, d = 6 m, h = 1.8 m and t = 0.12 m. This structure is solved by the energy method, and the results obtained are compared in Fig. 20 with the REC52 solution. The experimental results verified the numerical result of REC52 element, qualitatively.

6. Conclusions

A new functional based on the Gâteaux differential for folded plates with geometric and dynamic boundary conditions is presented. The mixed finite element REC52 is obtained in an explicit form. This rectangular element has four nodes and thirteen degrees of freedom per node. An interesting property of this formulation is observed in Eratlı and Aköz (1997): the numerical results converge from above and below depending on odd and even number of elements in the mesh refinement.

The following remarks result from theoretical consideration and numerical testing of folded plates:

· A new functional has been obtained based on the Gâteaux differential. This functional is very suitable for numerical methods, Aköz and Uzcan (Eratlı) (1992).
· The finite element method provides a general and systematic technique for constructing a basis, which is well-suited to irregular geometry. A mixed finite element based on this functional is used.
· There exists only first order derivatives in this functional. Therefore, linear shape functions are used and a mixed finite element REC52 can be obtained in an explicit form, and the resulting solution are not affected by shear locking.
· One of the big advantages of this formulation, forces and moments, which are the necessary unknowns in engineering problems, are obtained directly using the technique suggested here.
· As the use of the global co-ordinate system for the folded plates is complex and time consuming, the Lagrange Multiplier Method is used to interrelate the parameters assigned to nodes on the fold lines.
· Holographic and strain-gage tests are performed to verify the results of element REC52. The agreement numerical and experimental results are in good agrement.

References

Aköz, A.Y., Omurtag, M.H., and Doğruoğlu, A.N. (1991) "The mixed finite element formulation for three dimensional bars", *Int. J. Solids Structures*, **28**, 225-234.
Aköz, A.Y., and Uzcan (Eratlı), N. (1992), "The new functional for Reissner plates and its application", *Comp. & Struct.*, **44**(5), 1139-1144.
Aköz, A.Y., and Eratlı, N. (2000), "A sectorial element based on Reissner plate theory", *Struct. Eng. and Mech.*, **9**(6), 519-540.
Aköz, A.Y., and Özütok, A. (2000), "A functional for shells of arbitrary geometry and a mixed finite element method for parabolic and circular cylindrical shells", *Int. J. Numer. Methods in Eng.*, **47**, 1933-1981.
Belytschko, T., Tsay, C.S., and Liu, W.K. (1981), "A stabilization matrix for the bilinear Mindlin plate element", *Comp. Methods in Appl. Mech. and Eng.*, **29**, 313-327.
Develis and Reynolds (1967), *Theory and Applications of Holography*, Addison-Wesley Publishing Company.
Eratlı, N., and Aköz, A.Y. (1997), "The mixed finite element formulation for the thick plates on elastic foundations", *Comp. & Struct.*, **65**, 515-529.
Eratlı Uzcan, N. (1995), "Finite element formulation for folded plates", Ph.D. thesis (in Turkish), Dept. of Civil Engineering, Istanbul Technical University.
Huebner, K.H. (1975), *The Finite Element Method for Engineers*, John Wiles&Sons.

Hughes, T.J.R., Taylor, R.L., and Kanoknukkulchai, W. (1977), "A simple and efficient finite element for plate bending", *Int. J. Numer. Methods Eng.*, **11**, 1529-1543.

Iffland, J.S.B. (1979), "Folded plate structures", *J. Struct. Div.*, ASCE, **105**, ST1, 111-123.

Katılı, I. (1993a), "A new discrete Kirchhoff-Mindlin element based on Mindlin-Reissner plate theory and assumed shear strain fields-Part I:An extended DKT element for thick-plate bending analysis", *Int. J. Numer. Methods Eng.*, **36**, 1859-1883.

Katılı, I. (1993b), "A new discrete Kirchhoff-Mindlin element based on Mindlin-Reissner plate theory and assumed shear strain fields-Part II:An extended DKQ element for thick-plate bending analysis", *Int. J. Numer. Methods Eng.*, **36**, 1885-1908.

Lavy, Y., Bar-Yoseph, P., and Rosenhouse, G. (1992), "Mixed-hybrid finite strip method for folded plate structures", *Comp. & Struct.*, **42**(3), 433-446.

Mindlin, R.D. (1951), "The influence of rotatory inertia and shear on the flexural motions of elastic plates", *J. Appl. Mech.* ,ASME, **18**, 31-38.

Ohga, M., Shigematsu, T., and Kohigashi, S. (1991), "Analysis of folded plate structures by a combined boundary element-transfer matrix method", *Comp. & Struct.*, **41**(4), 739-744.

Özmen, G. (1963), "Solution of prismatic shells with energy method", *Ph.D. thesis* (in Turkish), Dept. of Civil Engineering, Istanbul Technical University.

Panc, V. (1975), *Theories of Elastic Plates*, Noordhoof International Publishing.

Pugh, E.D.L., Hinton, E., and Zienkiewicz, O.C. (1978), "A study of quadrilateral plate bending elements with reduced integration", *Int. J. Numer. Methods Eng.*, **12**, 1059-1079.

Reddy, J.N. (1986), *Applied Functional Analysis and Variational Methods in Engineering*, McGraw-Hill.

Reissner, E. (1946), "The effects of transverse shear deformation bending of elastic plates", *J. Appl. Mech.*, ASME, **12**, 69-77.

Report of the Task Committee on Folded Plate Construction Committee on Masonry and Reinforced Concrete Structural Division, Phase I Report on Folded Plate Construction, *J. Struct. Div.*, ASCE, **89**, ST6, 365-406, 1963.

Rockey, K.C., and Evans, H.R. (1967), "A finite element solution for folded plate structures", *Proc. of Conference on Space Structures*, Oxford, Blackwell, 165-188.

Stroke, G.W. (1968), *In Introduction to Coharvent Optics and Holography*, Academic Press.

Timoshenko, S. and Woinowisky-Krieger, S. (1959), *Theory of Plates and Shells*, McGraw-Hill.

Zienkiewicz, O.C., Taylor, R.L., and Too, J. (1971), "Reduced integration technique in general analysis of plates and shells", *Int. J. Numer. Methods Eng.*, **3**, 275-290.

Zienkiewicz, O.C., Bauer, J., Morgan, K., and Onate, E. (1977), "A simple and efficient element for axisymmetric shells", *Int. J. Numer. Methods Eng.*, **11**, 1545-1558.

Appendix I

Derivation concept of Eq. (1b) will be briefly reviewed. More information can be found at Panc 1975. The lateral stress σ_z can be found, assuming the parabolic shear stress distribution through the plate thickness and using equilibrium equation as follows,

$$\sigma_z = -\frac{q^2}{4}\left[2 - 3\left(\frac{2z}{h}\right) + \left(\frac{2z}{h}\right)^3\right]. \tag{A.1}$$

This stress distribution satisfies boundary conditions at $z = \mp h/2$, $\sigma_z = 0$, and $\sigma_z = -q$, respectively. Average rotation of cross-section Ω_x can be defined by employing energy argument as follow,

$$\Omega_x M_x = \int_{-h/2}^{h/2} \sigma_x u dz \tag{A.2}$$

where $u(z)$ is the displacement field through thickness. The stresses are related to the moment

$$\sigma_x = \frac{12M_x}{h^3}z \tag{A.3}$$

and by inserting (A.3) into (A.2), we obtain

$$\Omega_x = \frac{12}{h^3}\int_{-h/2}^{h/2} uzdz. \tag{A.4}$$

Taking derivative of (A.4), we obtain

$$\frac{\partial \Omega_x}{\partial x} = \frac{12}{h^3}\int_{-h/2}^{h/2} \frac{\partial u}{\partial x} zdz. \tag{A.5}$$

The stress-strain relations and moments definitions are

$$\varepsilon_x = \frac{\partial u}{\partial x} = \frac{1}{E}[\sigma_x - \mu(\sigma_y + \sigma_z)]$$

$$M_x = \int_{-h/2}^{h/2} \sigma_x zdz$$

$$M_y = \int_{-h/2}^{h/2} \sigma_y zdz \tag{A.6}$$

inserting (A.1) and (A.6) into (A.5), we obtain

$$\frac{\partial \Omega_x}{\partial x} = \frac{12}{Eh^3}\left[M_x - \mu M_y - \mu \frac{qh^2}{10}\right]. \tag{A.7}$$

The other relations can be obtained similarly.

Appendix II

Notation

M_x, M_y, M_{xy}	: moment components
Q_x, Q_y	: shear forces
N_x, N_y, N_{xy}	: in-plane force components
p, r, q	: distributed loads along the x, y, z axes, respectively
u, v, w	: displacements of plate along the x, y, z axes, respectively
Ω_x, Ω_y	: cross-sectional rotation of plates about x and y axes, respectively
h	: thickness of plate
E, μ, G	: modulus of elasticity, Poisson's ratio and shear modulus of elasticity respectively
$I_p(\mathbf{y})$, $I_l(\mathbf{y})$, $I_{fp}(\mathbf{y})$	: functionals of plate, in-plane element and folded plate, respectively
$[\ ,\ ]$	: inner product
$[\ ,\ ]_\varepsilon$	: geometric boundary condition
$[\ ,\ ]_\sigma$	: dynamic boundary condition
ψ_i	: shape functions (i = 1, ..., 4 for REC52)
ξ, η	: non-dimensional coordinates of a master element

Appendix III

γ coefficients and the submatrices $[k_1]$, $[k_2]$, $[k_3]$ in REC52 are defined as Eq. (A.8-A.12).

$$
\begin{aligned}
\gamma_1 &= 12/Eh^3,\\
\gamma_2 &= 2\mu/Eh^3,\\
\gamma_3 &= 12(1+\mu)/Eh^3,\\
\gamma_4 &= 12(1+\mu)/5Eh,\\
\gamma_5 &= 1/Eh,\\
\gamma_6 &= -\mu/Eh,\\
\gamma_7 &= 2(1+\mu)/Eh.
\end{aligned}
\tag{A.8}
$$

$$
[k_1] = \int_A \psi_i \psi_j dA = \begin{bmatrix} 4ab/9 & 4ab/18 & 4ab/18 & 4ab/36 \\ 4ab/18 & 4ab/9 & 4ab/36 & 4ab/18 \\ 4ab/18 & 4ab/36 & 4ab/9 & 4ab/18 \\ 4ab/36 & 4ab/18 & 4ab/18 & 4ab/9 \end{bmatrix},
\tag{A.9}
$$

$$
[k_2] = \int_A \frac{\partial \psi_i}{\partial x} \psi_j dA = \begin{bmatrix} -b/3 & -b/6 & -b/3 & -b/6 \\ -b/6 & -b/3 & -b/6 & -b/3 \\ b/3 & b/6 & b/3 & b/6 \\ b/6 & b/3 & b/6 & b/3 \end{bmatrix},
\tag{A.10}
$$

$$
[k_3] = \int_A \frac{\partial \psi_i}{\partial y} \psi_j dA = \begin{bmatrix} -a/3 & -a/3 & -a/6 & -a/6 \\ a/3 & a/3 & a/6 & a/6 \\ -a/6 & -a/6 & -a/3 & -a/6 \\ a/6 & a/6 & a/3 & a/6 \end{bmatrix}.
\tag{A.11}
$$

$$
\begin{array}{ccccccccccccc}
M_x & M_y & N_x & N_y & M_{xy} & N_{xy} & Q_x & Q_y & u & v & w & \Omega_x & \Omega_y \\
\downarrow & \downarrow & \downarrow & \downarrow & \downarrow & \downarrow & \downarrow & \downarrow & \downarrow & \downarrow & \downarrow & \downarrow & \downarrow
\end{array}
$$

$$
[k]_{fp} = \begin{bmatrix}
\gamma_1[k_1] & \gamma_2[k_1] & 0 & 0 & 0 & 0 & 0 & 0 & 0 & 0 & 0 & [k_2]^T & 0 \\
 & \gamma_1[k_1] & 0 & 0 & 0 & 0 & 0 & 0 & 0 & 0 & 0 & 0 & [k_3]^T \\
 & & \gamma_5[k_1] & \gamma_6[k_1] & 0 & 0 & 0 & 0 & [k_2] & 0 & 0 & 0 & 0 \\
 & & & \gamma_5[k_1] & 0 & 0 & 0 & 0 & 0 & [k_3] & 0 & 0 & 0 \\
 & & & & \gamma_3[k_1] & 0 & 0 & 0 & 0 & 0 & 0 & [k_3]^T & [k_2]^T \\
 & & & & & \gamma_7[k_1] & 0 & 0 & [k_3] & [k_2] & 0 & 0 & 0 \\
 & & & & & & \gamma_4[k_1] & 0 & 0 & 0 & [k_2]^T & [k_1] & 0 \\
 & & & & & & & \gamma_5[k_1] & 0 & 0 & [k_3]^T & 0 & [k_1] \\
 & & & & & & & & 0 & 0 & 0 & 0 & 0 \\
 & & \textit{Symmetrical} & & & & & & & 0 & 0 & 0 & 0 \\
 & & & & & & & & & & 0 & 0 & 0 \\
 & & & & & & & & & & & 0 & 0 \\
 & & & & & & & & & & & & 0
\end{bmatrix}
\tag{A.12}
$$